Controlled Ohmic and nonlinear electrical transport in inkjet-printed single-wall carbon nanotube films

Tero Mustonen,[1] Jani Mäklin,[1] Krisztián Kordás,[1] Niina Halonen,[1] Geza Tóth,[1] Sami Saukko,[1] Jouko Vähäkangas,[1] Heli Jantunen,[1] Swastik Kar,[2] Pulickel M. Ajayan,[2,3] Robert Vajtai,[4] Panu Helistö,[5] Heikki Seppä,[5] and Hannu Moilanen[6]

[1]*Microelectronics and Materials Physics Laboratories, Department of Electrical and Information Engineering, and EMPART Research Group of Infotech Oulu, University of Oulu, P.O. Box 4500, FIN-90014 Oulu, Finland*

[2]*Department of Materials Science and Engineering, Rensselaer Polytechnic Institute, Troy, New York 12180, USA*

[3]*Department of Mechanical Engineering and Materials Science, Rice University, Houston, Texas 77251-1892, USA*

[4]*Rensselaer Nanotechnology Center, Rensselaer Polytechnic Institute, Troy, New York 12180, USA*

[5]*Quantronics/Microtechnologies and Sensors, VTT Technical Research Centre of Finland, P.O. Box 1000, TT3, 02044 VTT Espoo, Finland*

[6]*LaserProbe LP Ltd., Jussintie 7, FIN-90800 Oulu, Finland*

(Received 19 October 2007; revised manuscript received 14 February 2008; published 26 March 2008)

We present the fabrication and characterization of logic elements (transistors and interconnects) built using our recently developed inkjet-printer-controlled deposition of single-wall carbon nanotube network films. The method requires no preselection of "metallic" or "semiconducting" nanotubes. By selecting the number of prints on a specified region, it is possible to have low-density, nonlinear, gate-voltage controllable transistors or high-density, linear, high-current-throughput metallic interconnects without any gate-voltage response. Intermediate steps drive the films between the nonlinear and linear regimes with precise controllability. The transport mechanism in these films as a function of bias, gate voltage, and temperature dependence have been investigated and analyzed using junction properties of metal-semiconductors in the context of networks of carbon nanotubes.

DOI: 10.1103/PhysRevB.77.125430 PACS number(s): 73.63.Fg, 73.30.+y, 73.50.−h

INTRODUCTION

Individual single-wall carbon nanotubes (SWCNTs) show fascinating electronic transport properties that depend on a number of factors such as nanotube chirality,[1–3] temperature,[4–7] electrical contact,[8–10] doping,[11] chemical functionalization,[12,13] and surrounding chemistry.[14,15] Individual nanotubes between metallic contacts with spacing up to several micrometers behave as ballistic conductors.[16,17] Coulomb blockade and single electron transport in nanotubes arranged in a back-gated field-effect transistor structure have been demonstrated at cryogenic temperatures.[18–20] At higher temperatures, metallic nanotubes with Ohmic contacts, fabricated with metals such as Pt, Pd, and Au, show a power law dependence of conductance and differential conductance on temperature and applied bias, respectively, proving previous theoretical predictions of Luttinger liquid behavior in nanotubes.[21,22] In contrast, a Schottky-type barrier builds up when semiconducting nanotubes are equipped with Ti or Al leads,[8,9,23] giving rise to activated and thermally assisted tunneling of charges into the nanotubes, which dominates the temperature dependence.

The picture is more complex when bundles of nanotubes or films of those with various geometries and degree of spatial alignment are considered, since the interaction of adjacent nanotubes in the film may lead to carrier screening effects,[23] hopping,[24–26] or even to a network of Schottky junctions as semiconducting and metallic tubes cross each other.[27–31] In spite of these factors, from an application perspective, bundles and/or large network configurations could be expected to "average" out the variations due to the above-mentioned parameters, and devices fabricated from such structures can be expected to remain more "reproducible" in their properties and performance, with higher throughput. Since, in many applications, the dimensions of electrodes are much larger than the diameter of individual nanotubes, scaling up the active elements between the electrodes using bundles and/or networks serves to enhance device-to-device reproducibility, in comparison to individual nanotubes, without compromising the overall device size.

In this work, we investigate the electronic transport properties of inkjet-printed, carboxyl functionalized SWCNT [SWCNT-$(COOH)_n$] networks between room temperature and 150 °C in ambient conditions as well as in nitrogen gas atmosphere. The films are deposited by inkjet printing between gold electrodes on alumina substrates (two-terminal measurements) and on customized Si chips (in back-gated field-effect transistor configurations). The fabrication method, which involves repetitive printing at the same locations, enables good control on film geometry (especially on the amount of nanotubes deposited on the substrate) and, therefore, current-voltage characteristics of nanotube films with well-defined average surface coverage (surface number density) could be acquired. We present the evolution of these current-voltage characteristics as a function of temperature for different surface coverages. We also demonstrate field-effect transistor behavior with inkjet deposited nanotube films of varying coverage, and highlight the effect of coverage on the transistor operation. These results complement previous findings of other research groups that were obtained from below-room-temperature measurements and contribute toward nanotube applications under realistic environmental conditions, such as sensors and cost-effective printed electronics.

TABLE I. Processing parameters of thin-film deposition and/or etching used in Si chip fabrication.

Material	Method	T (°C)	Chemistry	Flow rate (SCCM)	p (mTorr)	rf power (W)
SiO_2	PECVD	300	$SiH_4(5\%)+N_2/N_2O$	450/750	1000	15
Ti/Pt	Sputtering	215	Ar	16.8	8.9	200
SiO_2	Wet etch	25	$NH_4F+HF+H_2O$			
Pt	Wet etch	70	$HNO_3+HCl+H_2O$			
Ti	RIE	25	SF_6+O_2	20/20	20	20

EXPERIMENT

The SWCNT-COOHs that we used in our work were produced by electric arc discharge technique, then purified and functionalized in nitric acid [Sigma-Aldrich, carbon nanotube (CNT) content: 90%, carboxylic acid composition: 3–6 at. %, and bundle dimensions: 4–5 nm $\times 0.5$–1.5 μm].[32–34]

Inkjet printable aqueous solutions of CNTs are prepared as described elsewhere.[35,36] In a typical procedure, 2.5 mg of SWCNT-COOHs are dispersed in 20 ml de-ionized water by 30 min ultrasonic agitation. Subsequently, the solution is centrifuged at 3500 rpm for 10 min, and the supernatant solution is separated and centrifuged again. The centrifugation procedure is repeated until a stable dark brown solution is achieved. The as-obtained concentration of SWCNT-COOHs in water is ~ 0.1 g/L.

Printed lines of SWCNT-COOHs are deposited between thick-film gold electrodes (gap of ~ 200 μm) on alumina substrates[37] by using a material deposition printer (Dimatix DMP-2831, nominal drop volume of 10 pL and drop spacing of 25 μm). Nanotube films with different surface coverages on the substrates are achieved by printing different numbers of layers over the same pattern (3–20 layers).

The silicon chips were fabricated by standard thin-film process sequences including sputter deposition, plasma-enhanced chemical vapor deposition (PECVD), lithography, reactive ion etching (RIE), and wet etching (Table I). The nanotube solutions were printed by depositing individual droplets in the electrode area (Fig. 1).

Current-voltage curves were measured on each of the samples with a dual sourcemeter (Keithley 2612) in ambient air and in nitrogen atmosphere at temperatures from 20 to 150 °C.

RESULTS AND DISCUSSION

The nanotubes deposited on both types of test substrates form random networks of bundled SWCNTs with typical bundle length of ~ 0.5–2.0 μm and diameter of 10–20 nm as measured by transmission and scanning electron microscopy as well as by atomic force microscopy. The films are not perfectly homogeneous due to a stain ring formation at the perimeter of drying droplets caused by the pinning of the contact line and consequent outward capillary flow that carries particles to the edge.[38] The bundles are in intimate contact with the surface; however, in the case of the alumina substrate, the smaller surface voids at the boundaries of microscopic Al_2O_3 crystallites are bridged by suspended CNTs. The density of networks can be easily controlled by subsequent deposition steps on the same surface location as shown in Fig. 2. In the case of 20 prints, there is good coverage and the surface is conductive everywhere; while for the case of 3 prints, the high contrast features around some of the bundles indicate considerable charging by the electron beam, i.e., such films lack good percolation and grounding.

In devices based on individual semiconducting nanotubes, the contact plays a very significant role, since low-work-function metals form a Schottky interface, causing thermal

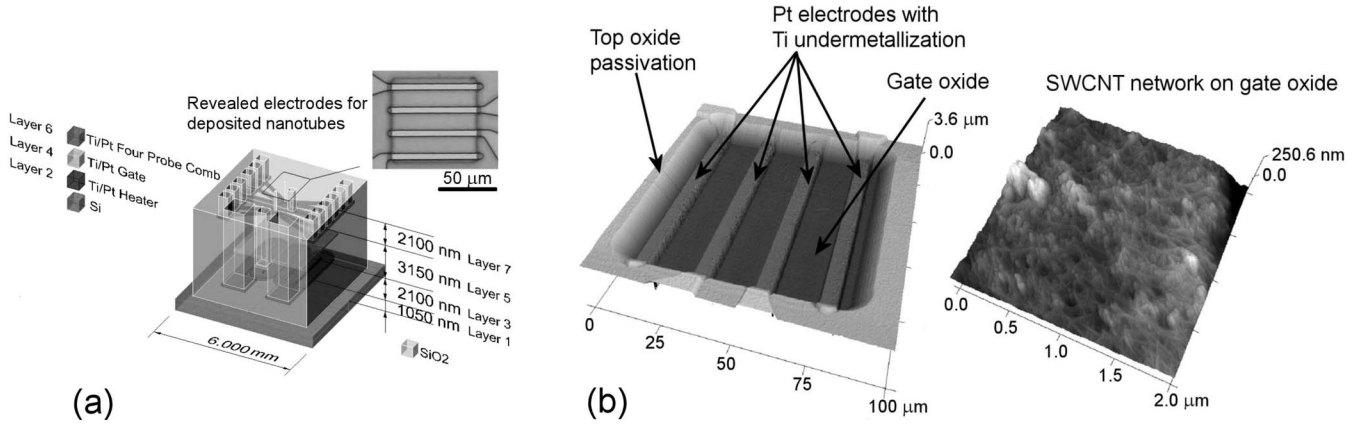

FIG. 1. (a) Layout of the Si chip used in the CNT thin-film FET measurements. The optical micrograph shows a set of Pt electrodes (source-drain) upon which the nanotube films were printed. (b) Atomic force microscopy images of the electrode area. The higher magnification image shows a network of nanotube bundles printed between the electrodes (on the gate oxide).

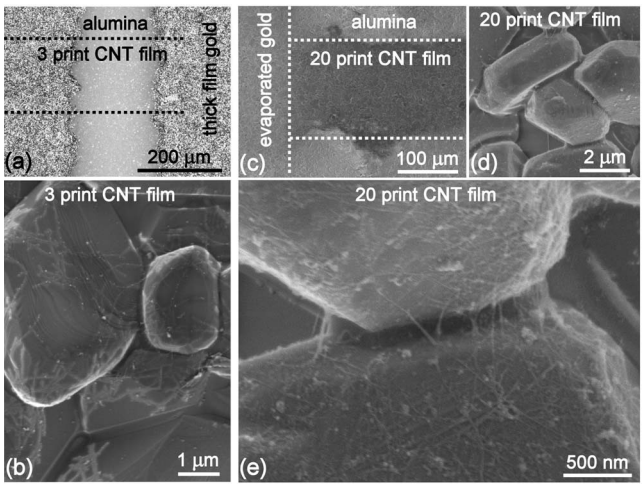

FIG. 2. Optical and scanning electron microscope images of the samples printed on alumina substrates. (a) Optical microscopy image of a low-density CNT line (three prints) connecting the gap between two gold electrodes. The dotted lines are to guide the eye along the edges of the printed nanotube pattern, which is practically invisible (Ref. 37). (b) Scanning electron microscope (SEM) picture shows a partially connected low-density network on the substrate. The high contrast features show local charge accumulation in the substrate around nonpercolated nanotubes. (c) Low magnification SEM image of a dense CNT line (20 prints) in the vicinity of a grounded gold electrode. Charging of the alumina substrate takes place where no nanotube network or evaporated metal film is deposited. (d) SEM image of a dense CNT network on alumina substrate and (e) close-up image of CNTs bridging two alumina crystallites. Note that because of the good percolation, the network is grounded well through the contact electrodes and local charging of the substrate by the electron beam is negligible as compared to that of the sample shown in (b).

emission to be the dominant mechanism for current injection at room temperature and above.[23,39,40] Thus, to avoid (or at least minimize) rectifying nanotube film-to-electrode contacts[8–10]—which might occur for very thin films if only semiconducting nanotubes are in direct contact with the metal leads—we used gold electrodes in our experiments.

Current-voltage (I-V) measurements performed on the films show coverage-dependent transport as shown in Fig. 3. A number of different samples with sheet resistivities between $k\Omega/\square$ to a few $M\Omega/\square$ were studied to estimate the reproducibility of I-V properties. The overall sample to sample variation of resistance for the same number of prints remained within a 30% deviation.[41] Nanotube films of higher density behave as Ohmic conductors characterized by linear I-V curves. This implies that higher surface coverage enables direct contact between the metallic SWCNTs in the tangled network, thus providing a continuous and highly conductive path for the current carriers to pass through. Accordingly, for dense networks, the I-V curves are expected to be linear with the slopes proportional to the nanotube surface coverage, which is in agreement with our experimental results. In contrast to the dense films, the less dense networks, which are obtained with lower numbers of print repetitions, show nonlinear features. With the decreased surface coverage, the probability of contiguous metallic nanotube network formation becomes lower and other (nonlinear) conduction processes contribute more significantly to the transport. Although in previous works using multiwalled carbon nanotubes the nonlinear I-V curves of low resistance films were explained by self-heating,[42,43] this would be very unlikely in our samples, since such an effect would be more pronounced for the denser films, where significantly higher power is generated compared to the less dense films. Anyhow, the I-V characteristics of thicker films are linear.[44]

In nanotube films, the network consists of metallic and semiconducting wires. Statistically, the amount of semiconducting nanotubes is twice as much as the metallic ones.[23,27] In sparse networks, only a few contiguous conduction paths exist, which are composed of a random sequence of both p-type semiconducting (s-CNT) and metallic carbon nanotubes (m-CNT). At the junctions of the two types of nanotubes, a Schottky-type potential barrier forms, since the valence band edge in s-CNTs lies below the Fermi energy of m-CNTs. In a simple picture, carriers that have energy larger than the barrier height will be injected via thermionic emission into the nanotube. In this picture, for a metal-semiconductor interface, the potential and temperature dependent current density $J(V,T)$ is described as[40]

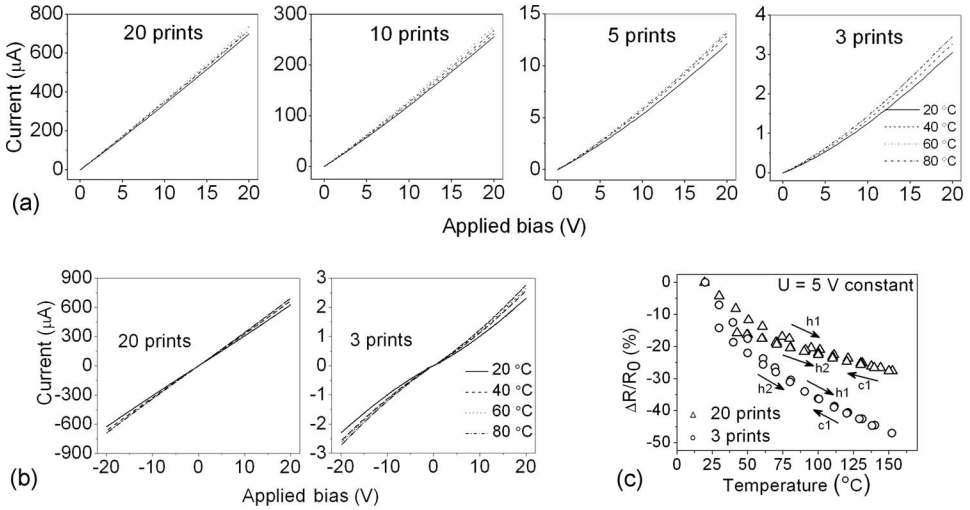

FIG. 3. Current-voltage characteristics of inkjet deposited SWCNT films of various coverage (print repetitions) at the temperature range of 20–80 °C measured (a) in ambient air and (b) in nitrogen atmosphere. (c) Relative change of film resistances $\Delta r/r_0$ of dense (20 prints) and sparse networks (3 prints) upon heating (h1) and subsequent cooling (c1) and reheating (h2) in nitrogen atmosphere up to 150 °C.

TABLE II. Apparent intrinsic resistance of the nanotube network R, effective barrier height Φ_b, and number of junctions m in series in a percolated path as a function of carbon nanotube surface coverage.

No. of prints	R (kΩ)	Φ_b (meV)	m
3	4875.0 ± 24.1	253.8 ± 3.0	66
5	1348.2 ± 17.1	220.0 ± 2.6	53
10	70.33 ± 0.29	148.6 ± 1.3	35
15	26.40 ± 0.03	117.9 ± 1.3	26
20	16.27 ± 0.01	107.0 ± 1.2	17

$$J(V,T) = A^*T^2 \exp\left(-\frac{\Phi_b}{kT}\right)\left[\exp\left(\frac{qV^*}{kT}\right) - 1\right], \quad (1)$$

where Φ_b is the Schottky barrier height, $A^* = 4\pi q m^* k^2/h^3$ is the Richardson constant, q is the elementary charge, $m^* = 0.037 m_e$ is the effective mass of the carriers,[45] and k and h are Boltzmann's and Planck's constants, respectively. The potential drop on the series intrinsic resistance R of CNTs is taken into account by considering $V^* = V - RI$, where R is the reciprocal of the I-V slope at large bias voltages. By applying Eq. (1) for a thin CNT film with A average cross section and m number of junctions along a percolated path, the current I becomes

$$I(V,T) = AA^*T^2 \exp\left(-\frac{\Phi_b}{kT}\right)\left[\exp\left(\frac{q(V-RI)/m}{kT}\right) - 1\right]. \quad (2)$$

The average area of cross section A can be estimated from the amount of CNTs deposited in the gap between the electrodes.[46] Now, by fitting Eq. (2) to the measured I-V plots, we get Φ_b and m parameters. For a film of three printed layers, the average barrier height is $\Phi_b \sim 254$ mV, which is reasonable considering a typical band gap of 300–900 mV for s-CNTs (Refs. 3, 39, and 47) and the corresponding Schottky barrier of 150–450 eV at the interface of semiconducting and metallic SWCNTs. The deduced barrier height is also in good agreement with the values (150–290 mV) of measurements performed on single junctions of metallic and semiconducting CNTs.[27,28] The number of Schottky junctions in series in a percolated path of $m \sim 66$ also gives a reasonable estimate since the distance between the electrodes (200 μm) is connected with CNT bundles having a length of ~ 1 μm. In the case of denser films, the calculated average barrier height gradually decreases with layer thickness. Also, the number of Schottky junctions involved in a percolation path decreases as the surface coverage gets higher since the metallic bundles or nanotubes cause parallel short circuits within a percolated path, enabling carriers to bypass the high resistance Schottky junctions (Table II). As a result of increased surface coverage or thickness, most charge carriers see a lowered effective barrier, which gives rise to pronounced linear I-V curves.

As shown in Figs. 3(a) and 3(b), the conductance of each sample increases with temperature. To analyze the temperature dependence, the sample resistances are measured in a nitrogen atmosphere at a constant 5 V bias and the relative change of resistance values $\Delta r/r_0$ are plotted as a function of temperature in Fig. 3(c). The resistance drop on the low-density network is higher than that on the thicker nanotube film. The reason for this difference is manifold and only a qualitative analysis of the current results is possible. In the sparse networks, we need to take into account the enhanced Schottky emission at the interfaces and also the increased carrier concentration in the semiconducting nanotubes as temperature is increased.[24–26,48,49] Accordingly, a negative temperature coefficient of resistance is expected for such sparse networks. In short (ballistic) metallic SWCNTs, electron-electron interactions can cause a very slow negative temperature coefficient of resistance,[21] whereas long (diffusive) metallic SWCNTs can show a positive temperature coefficient of resistance[50–52] caused by carrier scattering on radial breathing mode phonons.[53–55] We believe that in the case of the denser films, a combination of these two processes (due to the increasing metallic contribution to the overall transport) compensates for the large negative temperature coefficient of resistance seen in the (primarily semiconducting) sparse-network nanotube films. This results in a less negative temperature coefficient of resistance for the denser networks.

Besides the intrinsic properties of nanotubes, the effects of moieties that are adsorbed on the nanotubes also need consideration when measuring in a noninert atmosphere. As has been demonstrated elsewhere,[56,57] electron donors or proton acceptors adsorbed on nanotubes increase the electrical resistance because of the induced downshift of the valence band of the p-type nanotubes away from the Fermi level, by which hole depletion occurs and, consequently, the electrical conductivity decreases. To reveal the effect of adsorbed moieties on conduction, the resistances of both types of samples were also measured while cooling back to room temperature in the same nitrogen atmosphere as applied when heating. Both $\Delta r/r_0$ vs T curves split at ~ 100 °C and show lower values in the cooling ramp. When heating back again, the resistance of the samples follows the values obtained in the previous cooling ramps. These results indicate the presence of strongly adsorbed water on the nanotubes, which desorbed during the first heating cycle.[35,58]

It is worth pointing out that the picture is even more complex for carboxyl functionalized nanotubes because, besides the effect of absorbents, the functional groups and the adsorbed molecules on them also change the local distribution of carriers in the nanotubes.[59–62] Covalently bonded carboxyl functional groups increase the conductivity of the nanotubes due to the strong electron-withdrawing property of the functional group, viz. a partial positive charge appears around the carbon atom of the backbone that bonds the carboxyl group. Upon water exposure, a reduced electron-withdrawing power of the oxygen-containing defect groups leads to a reduced hole carrier concentration and, consequently, an increased resistance in the p-type nanotubes.[63]

The formation of Schottky junctions is known to pin the valence band of semiconducting CNTs close to the Fermi level of the metallic counterpart. The application of gate

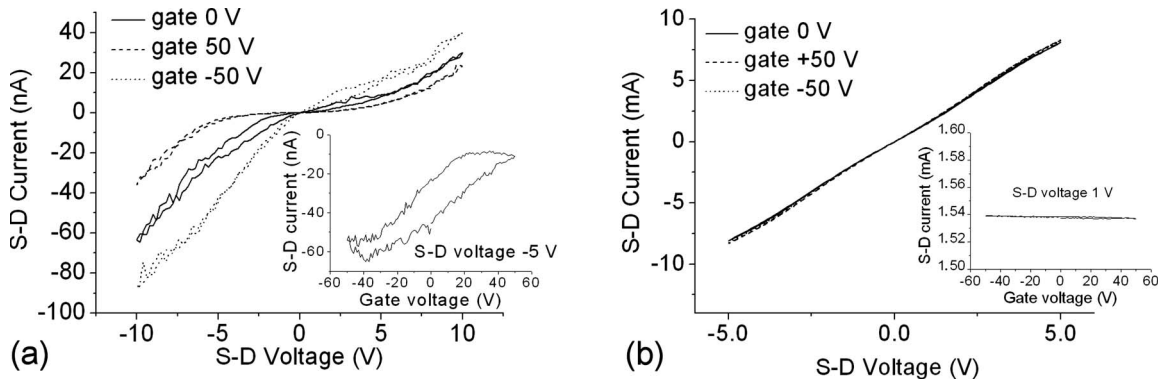

FIG. 4. I-V_{SD} and I-V_G sweeps on (a) diluted and (b) thick nanotube networks.

voltage causes band bending near the contacts, which can control the channel conductance by modulating the effective barrier visible to the injected charges, giving rise to a well known p-type transistor behavior. If the nonlinearities seen in the low-density devices are, indeed, from Schottky-type barriers, this would also show up as a p-type gate response. To demonstrate this, we have fabricated nanotube thin-film devices on a chip having a 3.15 μm gate oxide layer (SiO_2) above a thin-film Pt gate electrode. Nanotube films of various thicknesses were deposited on the top of the oxide layer between Pt electrodes of 15 μm gap to investigate I-V and transfer characteristics. Figure 4 shows the I-V and transfer characteristics of two such devices, (a) a low-density and a (b) high-density nanotube film field-effect transistor (FET). The low-density films show nonlinear I-V's, which could be modulated with the application of a gate voltage. The inset in Fig. 4(a) shows the gate response. FET structures with an on-off ratio of up to ~10 could be obtained in this way. The low switching ratio is attributed to the thicker gate oxide compared to those conventionally used in previous works and is expected to increase significantly with thinner gate oxides. The large hysteresis in the I-V_G suggests a considerable charge injection of carriers into the surrounding dielectric.[64–67] In contrast, a chip with a dense film of nanotubes was found to have linear I-V_{SD}. In agreement with the metallic nature of such films, a negligible gate effect could be seen.

CONCLUSIONS

To summarize, the fabrication of SWCNT films having controlled thickness is demonstrated by the means of inkjet printing of aqueous solutions of carboxyl functionalized nanotubes. Film-thickness-dependent conduction processes have been revealed and explained. In the case of low-density films, where a percolated network of s-CNT and m-CNT dominates, the electrical transport could be well explained by thermionic emission taking place at the junctions forming between crossing semiconducting and metallic CNTs. The conduction of the films becomes gradually Ohmic with increased thickness, which is attributed to the formation of a parallel metallic network of the deposited m-CNTs. We also demonstrate FET operation with thin films of inkjet-printed nanotubes acting as a p-type channel.[68–70]

The applications of carbon nanotubes in many low-size electronics still suffer from the absence of a simple method for "preselecting" semiconducting or metallic nanotubes (e.g., for transistors and interconnects, respectively).[71] We have demonstrated that the uncertainties in the overall metallic or semiconducting nature (in terms of the behavior of the I-V characteristics) when single or small bundles of nanotubes are used for device fabrication can be largely overcome by using films of carbon nanotube networks, with values of resistances within 30% reproducibility from device to device. This circumvents any tedious "preselection" of either individual metallic or semiconducting nanotubes typically needed for different kinds of applications. This method is very useful because it simply changes the surface coverage and barely affects the device size in any significant way. By controlling the number of prints on preselected regions, for example, it is easy to conceive "printed logic circuits" with transistors and interconnects all built from the same material, all at one go. The entire process is compatible with complementary metal-oxide-semiconductor, and by overlaying the prewritten circuits with insulators or dielectrics, three-dimensional stacked logic circuits can also be envisaged, with the dimensional limitations arising mainly from the drop size of the printer in use. We have also demonstrated that in typical operating conditions (300–450 K), our devices show a stable and reproducible performance (after the initial desorption of moieties), which is a necessary prerequisite for system integration. Our results complement well the existing experimental data published in the literature and provide important information about the deposition of SWCNT films with good control on layer thickness and, consequently, electrical transport. In addition, our results also highlight the significance of adsorbates as it alters the electrical behavior of the films in ambient conditions, which can be used to make sensors, and the reproducible temperature dependence can also be used to build thermometers.

ACKNOWLEDGMENTS

We acknowledge financial support from the Finnish Funding Agency for Technology and Innovation (Tekes, Project No. 1015/31/05)), the European Commission (FP6-2004-ISTNMP-3 STREP 017310 SANES), and the Interconnect Focus Center, one of the five FCR programs of the Semicon-

ductor Research Corporation, USA. R.V. acknowledges the NSEC Initiative of the NSF under Grant No. DMR-0117792. G.T. acknowledges the grants received from Nokia Foundation and from the Tekniikan edistämissäätiö (TES). K.K. is grateful to the Academy of Finland for the incentive funding received (120853). T.M. acknowledges the grants received from the Research Foundation of Seppo Säynäjäkangas, from the Tauno Tönning Foundation, and from the TES. We acknowledge the technical support from the Micro- and Nanotechnology Center, University of Oulu.

[1] M. S. Dresselhaus, G. Dresselhaus, and R. Saito, Phys. Rev. B **45**, 6234 (1992).
[2] J. W. Mintmire, B. I. Dunlap, and C. T. White, Phys. Rev. Lett. **68**, 631 (1992).
[3] Z. Wu, Z. Chen, X. Du, J. M. Logan, J. Sippel, M. Nikolou, K. Kamaras, J. R. Reynolds, D. B. Tanner, A. F. Hebard, and A. G. Rinzler, Transp. Sci. **305**, 1273 (2004).
[4] A. Thess, R. Lee, P. Nikolaev, H. Dai, P. Petit, J. Robert, C. Xu, Y. H. Lee, S. G. Kim, A. G. Rinzler, D. T. Colbert, G. E. Scuseria, D. Tománek, J. E. Fischer, and R. E. Smalley, Science **273**, 483 (1996).
[5] W. Ebbessen, H. J. Lezec, H. Hiura, J. W. Bennett, H. F. Ghaemi, and T. Thio, Nature (London) **382**, 54 (1996).
[6] H. Dai, E. W. Wong, and C. M. Lieber, Science **272**, 523 (1996).
[7] R. B. Capaz, C. D. Spataru, P. Tangney, M. L. Cohen, and S. G. Louie, Phys. Rev. Lett. **94**, 036801 (2005).
[8] P. Avouris, Chem. Phys. **281**, 429 (2002).
[9] A. Javey, J. Guo, Q. Wang, M. Lundstrom, and H. Dai, Nature (London) **424**, 654 (2003).
[10] H. M. Manohara, E. W. Wong, E. Schlect, B. D. Hunt, and P. H. Siegel, Nano Lett. **5**, 1469 (2005).
[11] C. Zhou, J. Kong, E. Yenilmez, and H. Dai, Science **290**, 1552 (2000).
[12] M. S. Strano, C. A. Dyke, M. L. Usrey, P. W. Barone, M. J. Allen, H. Shan, C. Kittrell, R. H. Hauge, J. M. Tour, and R. E. Smalley, Science **301**, 1519 (2003).
[13] J. Andzelm, N. Govind, and A. Maiti, Chem. Phys. Lett. **421**, 58 (2006).
[14] T. Yamada, Phys. Rev. B **69**, 125408 (2004).
[15] P. G. Collins, K. Bradley, M. Ishigami, and A. Zettl, Science **287**, 1801 (2000).
[16] D. Mann, A. Javey, J. Kong, Q. Wang, and H. Dai, Nano Lett. **3**, 1541 (2003).
[17] J.-Y. Park, S. Rosenblatt, Y. Yaish, V. Sazonova, H. Üstünel, S. Braig, T. A. Arias, P. W. Brouwer, and P. L. McEuen, Nano Lett. **4**, 517 (2004).
[18] C. Kane, L. Balents, and M. P. A. Fisher, Phys. Rev. Lett. **79**, 5086 (1997).
[19] S. J. Tans, M. H. Devoret, H. Dai, A. Thess, R. E. Smalley, L. J. Geerligs, and C. Dekker, Nature (London) **386**, 474 (1997).
[20] M. Bockrath, D. H. Cobden, P. L. McEuen, N. G. Chopra, A. Zettl, A. Thess, and R. E. Smalley, Science **275**, 1922 (1997).
[21] M. Bockrath, D. H. Cobden, J. Lu, A. G. Rinzler, R. E. Smalley, L. Balents, and P. L. McEuen, Nature (London) **397**, 598 (1999).
[22] R. Tarkiainen, M. Ahlskog, J. Penttilä, l. Roschier, P. Hakonen, M. Paalanen, and E. Sonin, Phys. Rev. B **64**, 195412 (2001).
[23] P. Avouris and J. Chen, Mater. Today **10**, 46 (2006).
[24] N. F. Mott and E. A. Davis, *Electronic Processes in Non-Crystalline Materials*, 2nd ed. (Clarendon, Oxford, 1979).
[25] A. B. Kaiser, Rep. Prog. Phys. **64**, 1 (2001).
[26] V. Skákalová, A. B. Kaiser, Y.-S. Woo, and S. Roth, Phys. Rev. B **74**, 085403 (2006).
[27] M. S. Fuhrer, Andrew K. L. Lim, L. Shih, U. Varadarajan, A. Zettl, and Paul L. McEuen, Physica E (Amsterdam) **6**, 868 (2000).
[28] Z. Yao, H. W. Ch. Postma, L. Balents, and C. Dekker, Nature (London) **402**, 273 (1999).
[29] R. Tamura, Physica B **323**, 211 (2002).
[30] M. Stadermann, S. J. Papadakis, M. R. Falvo, J. Novak, E. Snow, Q. Fu, J. Liu, Y. Fridman, J. J. Boland, R. Superfine, and S. Washburn, Phys. Rev. B **69**, 201402(R) (2004).
[31] A. A. Odintsov, Phys. Rev. Lett. **85**, 150 (2000).
[32] M. E. Itkis, D. E. Perea, S. Niyogi, J. Love, J. Tang, A. Yu, C. Kang, R. Jung, and R. C. Haddon, J. Phys. Chem. B **108**, 12770 (2004).
[33] C. Journet, W. K. Maser, P. Bernier, A. Loiseau, M. L. de la Chapelle, S. Lefrant, P. Deniard, R. Lee, and J. E. Fischer, Nature (London) **388**, 756 (1997).
[34] B. Zhao, H. Hu, and R. C. Haddon, Adv. Funct. Mater. **14**, 71 (2004).
[35] K. Kordás, T. Mustonen, G. Tóth, H. Jantunen, M. Lajunen, C. Soldano, S. Talapatra, S. Kar, R. Vajtai, and P. M. Ajayan, Small **2**, 1021 (2006).
[36] T. Mustonen, K. Kordás, S. Saukko, G. Tóth, J. S. Penttilä, P. Helistö, H. Seppä, and H. Jantunen, Phys. Status Solidi B **244**, 4336 (2007).
[37] The printed films are highly transparent in the visible wavelengths. For the three prints (on glass), the film has an optical transparency of $\sim$0.98, which slightly decreases as more prints are applied ($T \sim 0.88$ for 20 prints).
[38] R. D. Deegan, O. Bakajin, T. F. Dupont, G. Huber, S. R. Nagel, and T. A. Witten, Nature (London) **389**, 827 (1997).
[39] J. Appenzeller, M. Radosavljevic, J. Knoch and Ph. Avouris, Phys. Rev. Lett. **92**, 048301 (2004).
[40] S. M. Sze, *Physics of Semiconductor Devices* (Wiley, New York, 1981).
[41] In the case of batch-to-batch fabrication, variation of results might occur also due to several factors such as printing nozzle clogging, nanotube quality, degree of functionalization, ink concentration, ink rheology, and shelf time (bundling and precipitation increase in storage). However, it is important to note that these uncertainties have no roots in the suggested technique and can be avoided by proper optimization and standardization of the technology in the future.
[42] B. Q. Wei, R. Spolenak, P. Kohler-Redlich, M. Rühle, and E. Arzt, Appl. Phys. Lett. **74**, 3149 (1999).
[43] C. H. Liu and S. S. Fan, Appl. Phys. Lett. **90**, 041905 (2007).
[44] If we assume an inhomogeneous nanotube distribution on the substrate, which is actually close to reality, one might argue the

strongly localized heat that is dissipated exclusively along the percolated conduction paths. To show that self-heating is not responsible for the nonlinear behavior, let us consider a highly resistive film (nonlinear *I-V*) with n number of percolated channels, which are parallel to each other, e.g., five prints of 1.9 MΩ that dissipate ~53 μW power at 10 V applied bias, i.e., $\sim 53/n$ μW in each path. Next we compare this to a film (linear *I-V*) with much better conductivity, say, 15 prints of 29.5 kΩ that dissipate 3.4 mW power at 10 V bias. From the ratio of the two resistances 1.9 MΩ/29.5 kΩ ~ 64, a reasonable estimate of the percolated parallel conduction paths in the thicker film is obtained ($64n$). This gives an average of $\sim 53/n$ μW power dissipation in each conduction path, i.e., the local heat dissipation for the two films having different *I-V* characteristics is practically the same. Therefore, the nonlinearity of the *I-V* curves should originate from processes other than the local self-heating.

[45] P. Jarillo-Herrero, S. Sapmaz, C. Dekker, L. P. Kouwenhoven, and H. S. J. van der Zant, Nature (London) **429**, 389 (2004).

[46] We assume that the area of each junction in the film is the same as the cross-section area of the nanotubes or bundles forming the junction. The amount of SWCNTs in the printouts is estimated from the drop volume (10 pL), drop spacing (25 μm), and concentration of ink (0.1 g/L=1 pg/drop). The printed area between the electrodes is 200×200 μm^2, requiring 64 drops in a single layer. The printed amount of SWCNTs thus becomes $\sim 64 \times 10^{-12}$ g, which results in an average nanotube coverage of $\sim 16 \times 10^{-16}$ g/μm^2 on the substrate. Assuming a 1.4 g/cm^3 density for the nanotube bundles, the printed volume is ~46 μm^3, corresponding to a cross-section area of 0.23 μm^2 or to an average film thickness of 1.1 nm in a single printout.

[47] R. Bruce Weisman and Sergei M. Bachilo, Nano Lett. **3**, 1235 (2003).

[48] B. Kaiser, G. Düsberg, and S. Roth, Phys. Rev. B **57**, 1418 (1998).

[49] J. E. Fischer, H. Dai, A. Thess, R. Lee, N. M. Hanjani, D. L. Dehaas, and R. E. Smalley, Phys. Rev. B **55**, R4921 (1997).

[50] For thick films of SWCNTs such as as-grown mats and bucky papers (which obviously have linear *I-V* properties similar to our dense networks), the temperature coefficient of resistivity $\partial\rho/\partial T$ is not necessarily positive as for ordinary metals. It is, in fact, typically negative for low temperatures and positive only at higher temperatures. The turn-back point varies from sample to sample and depends on the method of nanotube synthesis and treatment. For details, see also Refs. 26, 48, 49, 51, and 52.

[51] R. Gaál, J.-P. Salvetat, and L. Forró, Phys. Rev. B **61**, 7320 (2000).

[52] A. G. Rinzler, J. Liu, H. Dai, P. Nikolaev, C. B. Huffman, F. J. Rodrígez-Macías, P. J. Boul, A. H. Lu, D. Heymann, D. T. Colbert, R. S. Lee, J. E. Fischer, A. M. Rao, P. C. Ecklund, and R. E. Smalley, Appl. Phys. A: Mater. Sci. Process. **67**, 29 (1998).

[53] B. F. Habenicht, C. F. Craig, and O. V. Prezhdo, Phys. Rev. Lett. **96**, 187401 (2006).

[54] Y. Yin, A. N. Vamivakas, A. G. Walsh, S. B. Cronin, M. S. Ünlü, B. B Goldberg, and A. K. Swan, Phys. Rev. Lett. **98**, 037404 (2007).

[55] A. Hartschuh, H. N. Pedrosa, L. Novotny, and T. D. Krauss, Science **301**, 1354 (2003).

[56] J. Kong, N. R. Franklin, C. Zhou, M. G. Chapline, S. Peng, K. Cho, and H. Dai, Science **287**, 622 (2000).

[57] J. Zhao, A. Buldum, J. Han, and J. P. Lu, Nanotechnology **13**, 195 (2002).

[58] K. Parikh, K. Cattanach, R. Rao, D.-S. Suh, A. Wu, and S. K. Manohar, Sens. Actuators B **113**, 55 (2006).

[59] U. Dettlaff-Weglikowska, V. Skákalová, R. Graupner, S. H. Jhang, B. H. Kim, H. J. Lee, L. Ley, Y. W. Park, S. Berber, D. Tománek, and S. Roth, J. Am. Chem. Soc. **127**, 5125 (2005).

[60] G. Fanchini, H. E. Unalan, and M. Chhowalla, Appl. Phys. Lett. **90**, 092114 (2007).

[61] M. Burghard and K. Balasubramanian, Small **1**, 180 (2005).

[62] M. Burghard, Surf. Sci. Rep. **58**, 1 (2005).

[63] P. C. P. Watts, N. Mureau, Z. Tang, Y. Miyajima, J. D. Carey, and S. R. P. Silva, Nanotechnology **18**, 175701 (2007).

[64] A. Vijayaraghavan, S. Kar, C. Soldano, S. Talapatra, O. Nalamasu, and P. M. Ajayan, Appl. Phys. Lett. **89**, 162108 (2006).

[65] S. Kar, A. Vijayaraghavan, C. Soldano, S. Talapatra, R. Vajtai, O. Nalamasu, and P. M. Ajayan, Appl. Phys. Lett. **89**, 132118 (2006).

[66] M. S. Fuhrer, B. M. Kim, T. Dürkop, and T. Brintlinger, Nano Lett. **2**, 755 (2002).

[67] M. Radosavljević, M. Freitag, K. V. Thadani, and A. T. Johnson, Nano Lett. **2**, 761 (2002).

[68] N. Pimparkar, Q. Cao, S. Kumar, J. Y. Murthy, J. Rogers, and M. A. Alam, IEEE Electron Device Lett. **28**, 157 (2007).

[69] G. Gruner, J. Mater. Chem. **16**, 3533 (2006).

[70] J. Vaillancourt, X. Lu, X. Han, and D. C. Janzen, Electron. Lett. **42**, 23 (2006).

[71] J. Robertson, Mater. Today **10**, 46 (2004).